TICAM Report 02-32

GOAL-ORIENTED *hp*-ADAPTIVITY FOR ELLIPTIC PROBLEMS

P. Solin, L. Demkowicz

Texas Institute for Computational and Applied Mathematics
The University of Texas at Austin
Austin, TX 78712

August 2002

Abstract

We propose and test a fully automatic, goal-oriented *hp*-adaptive strategy for elliptic problems. The method combines two techniques: the standard goal-oriented adaptivity based on a simultaneous solution of a dual problem, and a recently proposed *hp*-strategy based on minimizing the projection-based interpolation error of a reference solution. The proposed strategy is illustrated with two numerical examples: Laplace equation in L-shape domain, and an axisymmetric Maxwell problem involving radiation of a loop antenna wrapped around a metallic cylinder into a conductive medium.

Key words: *hp* finite elements, *hp*-adaptivity, dual problem, goal-oriented adaptivity
AMS subject classification: 65N30, 35L15

Acknowledgment

The work of the first author has been supported with TICAM postdoctoral fellowship, and of the second author by Air Force under Contract F49620-98-1-0255.

1 Introduction

The research presented in this paper is a continuation of the study on a fully automatic *hp*-adaptivity for elliptic problems in energy norm [8]. One of the main advantages of this strategy is that it does not need to use an a-priori information about singularities of the solution for the construction of the initial mesh. It has been documented in [8] that the strategy is capable of delivering exponential convergence rates and optimal meshes in the

full range of error level, especially also in the *preasymptotic* range. The algorithm is based on the solution of the problem on a globally refined *hp*-mesh, and on the construction of a next optimal *hp*-mesh which minimizes the projection-based interpolation error of the fine grid solution.

The idea of adding the solution of the dual problem to this strategy is motivated by several practical examples, a representative of which is presented in paragraph 1.1.

Before we bring together the goal-oriented adaptivity and *hp*-adaptivity proposing a new adaptive strategy in section 2, we shortly review the basic principles of each of them separately in paragraphs 1.2 and 1.3. In paragraph 1.4, a special attention is given to the mesh optimization procedure which is the very core of the fully-automatic algorithm.

In section 3 we solve a model elliptic problem (Laplace equation in the L-shape domain) and in section 4 we come back to the problem introduced in paragraph 1.1. Conclusions and outlook for future work are drawn in section 5.

1.1 A motivating problem: Radiation from a loop antenna

We are concerned with the solution of the standard model radiation problem relevant to drilling technologies, [10]. The problem is illustrated in Fig. 1. A loop antenna, wrapped around an infinite metallic cylinder, radiates into a conductive homogeneous medium.

The problem consists in solving the time-harmonic Maxwell's equations,

$$\boldsymbol{\nabla} \times \left(\frac{1}{\mu} \boldsymbol{\nabla} \times \boldsymbol{E} \right) - (\omega^2 \epsilon - \jmath \omega \sigma) \boldsymbol{E} = 0, \tag{1.1}$$

to be satisfied in the whole space minus domain D occupied by the loop antenna, with a prescribed impressed surface current on the surface of the antenna,

$$\boldsymbol{n} \times \left(\frac{1}{\mu} \boldsymbol{\nabla} \times \boldsymbol{E} \right) = -\jmath \omega \boldsymbol{J}_s^{imp}. \tag{1.2}$$

We choose to model the antenna with a surface rather than volume current (Neumann boundary condition instead of a source term) to avoid unnecessary refinements in the domain occupied by the antenna.

The standard variational formulation reads as follows [16]

$$\int_{\mathbf{R}^3 \setminus D} \frac{1}{\mu} \boldsymbol{\nabla} \times \boldsymbol{E} \cdot \boldsymbol{\nabla} \times \boldsymbol{F} - \int_{\mathbf{R}^3 \setminus D} (\omega^2 \epsilon - \jmath \omega \sigma) \boldsymbol{E} \cdot \boldsymbol{F} = -\jmath \omega \int_{\partial D} \boldsymbol{J}_s^{imp} \cdot \boldsymbol{F}, \tag{1.3}$$

for every test function $\boldsymbol{F}$, with $\boldsymbol{E}$ and $\boldsymbol{F}$ satisfying appropriate boundary conditions at infinity and ∂D denoting the boundary of domain D occupied by the antenna. Two essential simplifications can be made:

- Due to the axisymmetry of the problem, components $E_r = E_z = 0$ and $E = E_\varphi = E_\varphi(r, z)$ (in the sequel we leave out the index φ for tangential component of $\boldsymbol{E}$).

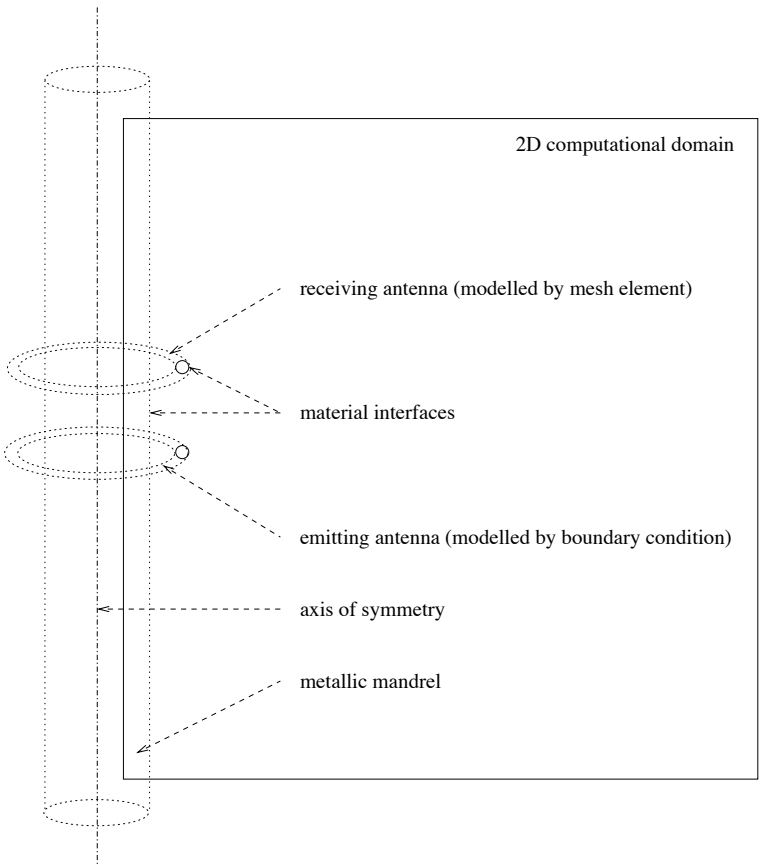

Figure 1: Basic arrangement of the device and computational domain (with adjusted scaling in the r-direction). The actual measures are given in paragraph 1.1.1.

- Due to the exponential decay of the solution away from the antenna, the resulting two-dimensional problem for E can be stated in a bounded rectangular domain Ω shown in Fig. 1, encompassing a portion of the metallic mandrel terminated away from $r = 0$. The equation is accompanied with a homogeneous Dirichlet boundary condition on the truncating boundary Γ.

The ultimate 2D variational problem, stated in polar coordinates (r, z) reads as follows:

$$\begin{cases} E = 0 \text{ on } \Gamma \\ \displaystyle\int_\Omega \left\{ \frac{1}{\mu} \left[\frac{\partial E}{\partial z}\frac{\partial \boldsymbol{v}}{\partial z} + \frac{1}{r^2}\left(E + r\frac{\partial E}{\partial r}\right)\left(\boldsymbol{v} + r\frac{\partial \boldsymbol{v}}{\partial r}\right)\right] - (\omega^2\epsilon - \jmath\omega\sigma)E\boldsymbol{v} \right\} r \,\mathrm{d}r\mathrm{d}z \\ = \jmath\omega \displaystyle\int_{\partial D} r\boldsymbol{J}_s^{imp} \cdot \boldsymbol{v} \,\mathrm{d}s, \qquad \text{for every test function } \boldsymbol{v}, \boldsymbol{v} = 0 \text{ on } \Gamma. \end{cases} \tag{1.4}$$

(Here $\mathrm{d}s^2 = \mathrm{d}r^2 + \mathrm{d}z^2$)

Notice that the original Neumann boundary condition on Γ translates now into a Cauchy (Robin) boundary condition,

$$\frac{\partial E}{\partial r} + \frac{n_r}{r} E = \jmath\omega \boldsymbol{J}_s^{imp} \tag{1.5}$$

where $\boldsymbol{n} = (n_r, n_z)^T$.

1.1.1 Goal of computation

Besides the emitting antenna, a receiving antenna, occupying another subdomain $D_1 \subset \Omega$ is placed into the computational domain. Our task is to compute the value

$$N(E) = 20 \log_{10} \int_{D_1} Er \, \mathrm{d}r\mathrm{d}z \tag{1.6}$$

representing a measure to the electromagnetic force at the receiving antenna, measured in dB.

We shall describe now the geometry of the domain in more detail. All values are given in meters (some of them being converted from inches...).

Both antennas have identical form of a single axisymmetric ring of radius $r_a = 0.03048$. The cross-section of the antennas is circular with radius $r_c = 0.000718$. Midpoints of the emitting and receiving antenna in the axisymmetric geometry are $P_0 = [0.03048, 0]$ and $P_1 = [0.03048, 0.5]$, respectively.

Recall that we model the emitting antenna by means of a Cauchy boundary condition for E in order to avoid refinements in its interior. Hence, our computational domain Ω is obtained after subtracting the emitting antenna (i.e. circle with the midpoint P_0 and radius r_c) from the rectangle $[0.02, 2.0] \times [-2.0, 2.0]$. The subdomain $\Omega_m \subset \Omega$, $\Omega_m = [0.02, 0.0254] \times [-2.0, 2.0]$ represents a metallic mandrel with the material properties $\mu = 1$, $\sigma = 10^7$, $\epsilon = 1$. The same material properties are chosen also for the receiving antenna. The rest of Ω represents mud and soil with the material properties $\mu = 1$, $\sigma = 1$, $\epsilon = 1$. Here μ stands for the permeability, σ for the electrical conductivity and ϵ for the dielectric constant.

The frequency and angular frequency of the harmonic field have the values $f = 2.10^6$, $\omega = 2\pi f$. The computational domain with the initial mesh is shown in Fig. 2. Grid points in the r- and z-direction are listed in Tables 1 and 2, respectively.

0.02	0.0254	0.029214	0.030226	0.030734
0.031746	0.03738	0.075042	0.326024	2.0

Table 1: Grid points in the r-direction.

We impose certain geometrical gradation of the mesh towards the antennas in order to minimize the initial mesh error. Let us remark that the shape of the initial mesh influences the convergence of adaptive schemes in a non-negligible way.

-2.0	-0.500254	-0.499746	-0.044248	-0.007003
-0.001266	-0.000254	0.000254	0.001266	0.007003
0.044248	0.455752	0.492997	0.498734	0.499746
0.500254	0.501266	0.507003	0.544248	2.0

Table 2: Grid points in the z-direction.

It turns out that it is extremely difficult to resolve this problem with a sufficiently high accuracy using schemes which are h- or hp-adaptive in a global energy norm.

1.2 Basic principles of goal-oriented adaptivity

During the last decade, goal-oriented adaptivity for PDE's has been a topic of permanent scientific and engineering interest, and several basic methodologies have been proposed (see, e.g., [3, 4, 17, 5, 13, 14, 2]). In comparison with the adaptivity in energy norm which attempts to minimize the energy of the residual of the approximate solution, the goal-oriented approach attempts to control concrete features of the solved problem (*quantities of interest*). Goal-oriented adaptive techniques are designed to achieve precise resolution in quantities of interest with significantly less degrees of freedom than the standard adaptive schemes.

Quantities of interest can be represented, e.g., as bounded linear functionals of the solution. The goal in the motivating problem from the previous paragraph leads to a functional of the type

$$L(\boldsymbol{u}) = \int_{\Omega_s} \boldsymbol{u}(x)\mathrm{d}x \tag{1.7}$$

where Ω_s is a subdomain of the computational domain Ω. For vector-valued solutions, we may be interested, e.g., in the flux through the boundary of a subdomain Ω_s of Ω:

$$L(\boldsymbol{u}) = \int_{\partial\Omega_s} \boldsymbol{u}(x)\cdot\boldsymbol{n}(x)\mathrm{d}S = \int_{\Omega_s} \nabla\cdot\boldsymbol{u}(x)\mathrm{d}x. \tag{1.8}$$

However, there are numerous quantities of interest which cannot be directly expressed in terms of bounded linear functionals. A particularly important example is the value of the solution $\boldsymbol{u}$ at a selected point x_0 in domain Ω. In such cases we may try to find a suitable approximation of the quantity of interest, e.g.,

$$L(\boldsymbol{u}) = \frac{1}{|B(x_0,r)|}\int_{B(x_0,r)} \boldsymbol{u}(x)\mathrm{d}x \tag{1.9}$$

where $B(x_0,r)\subset\Omega$ is a ball with the center x_0 and a sufficiently small radius r. Another possible approach to pointwise values is the use of regularizing *mollifiers* (see, e.g. [12]).

Let us recall the basic ideas of the goal-oriented adaptivity leading to the formulation and solution of the dual problem:

- Consider a problem to find a solution $\boldsymbol{u}$ lying in a Hilbert space V and satisfying the weak fomulation
$$b(\boldsymbol{u}, \boldsymbol{v}) = f(\boldsymbol{v}) \tag{1.10}$$
for all $\boldsymbol{v} \in V$, b being an elliptic bilinear form defined on $V \times V$ and $f \in V'$.

- Consider the discrete problem
$$b(\boldsymbol{u}_{h,p}, \boldsymbol{v}_{h,p}) = f(\boldsymbol{v}_{h,p}) \tag{1.11}$$
for all $\boldsymbol{v}_{h,p} \in V_{h,p}$ where $V_{h,p} \subset V$ is a polynomial finite element approximation of space V.

- Define the error $\boldsymbol{e}_{h,p} = \boldsymbol{u} - \boldsymbol{u}_{h,p}$ and consider the residual
$$\boldsymbol{r}_{h,p}(\boldsymbol{v}_{h,p}) = f(\boldsymbol{v}_{h,p}) - b(\boldsymbol{u}_{h,p}, \boldsymbol{v}_{h,p}). \tag{1.12}$$

- Relate the residual $\boldsymbol{r}_{h,p}$ to the error in the quantity of interest, i.e. find $G \in V''$ such that
$$G(\boldsymbol{r}_{h,p}) = L(\boldsymbol{e}_{h,p}).$$

- By reflexivity, G can be related to an element $\boldsymbol{v}$ in the original space (*influence function*),
$$G(\boldsymbol{r}_{h,p}) = \boldsymbol{r}_{h,p}(\boldsymbol{v}) = f(\boldsymbol{v}) - b(\boldsymbol{u}_{h,p}, \boldsymbol{v}) = b(\boldsymbol{u}, \boldsymbol{v}) - b(\boldsymbol{u}_{h,p}, \boldsymbol{v}) = \underbrace{b(\boldsymbol{e}_{h,p}, \boldsymbol{v}) = L(\boldsymbol{e}_{h,p})}$$
where $\boldsymbol{v}$ is the solution to the *dual problem*:

- Find $\boldsymbol{v} \in V$ such that
$$b(\boldsymbol{u}, \boldsymbol{v}) = L(\boldsymbol{u}) \tag{1.13}$$
for all $\boldsymbol{u} \in V$.

- Consider the discrete dual problem
$$b(\boldsymbol{u}_{h,p}, \boldsymbol{v}_{h,p}) = L(\boldsymbol{u}_{h,p}) \tag{1.14}$$
for all $\boldsymbol{u}_{h,p} \in V_{h,p}$.

- Estimate the error in the quantity of interest by means of the errors *in energy norms* for both the direct and dual problem:
$$|L(\boldsymbol{u}) - L(\boldsymbol{u}_{h,p})| = |L(\boldsymbol{u} - \boldsymbol{u}_{h,p})| = |b(\boldsymbol{u} - \boldsymbol{u}_{h,p}, \boldsymbol{v})| = |b(\boldsymbol{u} - \boldsymbol{u}_{h,p}, \boldsymbol{v} - \boldsymbol{v}_{h,p})| \leq \tag{1.15}$$
$$\leq \sum_{K \in \mathcal{T}_{h,p}} ||\boldsymbol{u} - \boldsymbol{u}_{h,p}||_{e,K} ||\boldsymbol{v} - \boldsymbol{v}_{h,p}||_{e,K}.$$
(Standard orthogonality property for the error in the solution was used.)

1.3 Brief review of *hp*-adaptivity

The *hp*-version of the finite element method combines the adaptivity in h (spatial refinements) with the adaptivity in p (variation of the degree of polynomial approximation in finite elements) in a unique way. The basic advantage with respect to other h- or p- only adaptive schemes is based on the fact that the method achieves an exponential convergence in the energy norm for linear elliptic boundary value problems with possibly singular solutions. In other words, as opposed to h- and p-methods, the simultaneous refinements in both h and p allow to concentrate the degrees of freedom at singularities in a way which is sufficient to control them numerically. Such singularities are natural for domains with re-entrant corners, for points on the boundary where the boundary conditions change their type, and intersections of material interfaces. Their efficient resolution is crucial in many practical problems arizing in the engineering practice.

Nowadays, the theory of the *hp*-version of the finite element method is well-established and founded on solid results mostly due to the efforts of Babuška and coworkers. However, the practical realization of fully automatic and robust 3D *hp*-adaptive algorithms still presents many serious difficulties mainly due to excessive programming complexity. We refer to [8, 6, 15].

1.4 Mesh optimization procedure

An adaptive finite element strategy is always based on some information about the local approximation error that decides where the finite element mesh is to be refined. Most approaches are based on the evaluation of error estimators of various kinds on each mesh element. This seems to be sufficient for schemes which are adaptive either in h or in p only, because it is only the magnitude of the error in an element which decides about the refinement of the element. However, the *hp*-adaptivity brings more choices for an element to be refined: there is the possibility to perform either a p-refinement only, or to split the element spatially with various distributions of the polynomial degree p for its sons. Obviously, we must be critical when deciding between various refinement possibilities, which means that we must take into account both the invested number of degrees of freedom and the profit which the various refinement options bring. Such refinement options for a mesh element are called *competitive element refinements*.

An original approach based on the maximization of the decrease rate for the local *hp*-interpolation error with respect to a *reference solution* was presented in [15]. A reference solution $\boldsymbol{u}_{ref}$ is an approximation of the exact solution u which is closer to the exact solution than the original approximation $\boldsymbol{u}_{h,p}$. Hence, the difference $\boldsymbol{u}_{ref} - \boldsymbol{u}_{h,p}$ is capable of delivering useful information not only about the magnitude but also about the concrete *shape* of the error $\boldsymbol{e}_{h,p}$. The reference function can be obtained in several different ways (see, e.g., [15] where for this purpose Babuška's *extraction formulas* were used).

In [8], reference solution is computed as an approximate solution corresponding to an hp-grid obtained by a uniform h- and p-refinement such that $h \to h/2$ and $p \to p+1$ for all mesh elements. By $\boldsymbol{u}_{h/2,p+1}$ we denote the fine grid solution.

Let us remark that for h-adaptivity the fine mesh is constructed by uniform h-refinement only. This is sufficient as, in this case, the variation in p is not involved in the mesh optimization process.

It is our aim to minimize the error in energy norm

$$||\boldsymbol{e}||_e^2 = ||\boldsymbol{u} - \boldsymbol{u}_{h,p}||_e^2. \tag{1.16}$$

In the language of element contributions we can write

$$||\boldsymbol{u} - \boldsymbol{u}_{h,p}||_e^2 \leq \sum_{K \in \mathcal{T}_{h,p}} ||\boldsymbol{u} - \boldsymbol{u}_{h,p}||_{e,K}^2, \tag{1.17}$$

where $\mathcal{T}_{h,p}$ stands for the hp-mesh and K for a mesh element. Obviously the minimization of $||\boldsymbol{u} - \boldsymbol{u}_{h,p}||_{e,K}^2$ cannot be done locally. But, asymptotically, we can achieve the same goal by minimizing

$$||\boldsymbol{u}_{ref} - \Pi_{h,p}\boldsymbol{u}_{ref}||_{e,K}^2 \tag{1.18}$$

on all $K \in \mathcal{T}_{h,p}$, where $\Pi_{h,p}$ is a suitable *projection-based interpolation*. The projection-based interpolation must satisfy the following conditions, see [7],

- the interpolant must lie in the finite element space,
- the interpolation must be *local*, i.e. it must be capable of projecting a function onto an element using only information accessible from inside of the element,
- the interpolation must be *optimal*, i.e. deliver the same convergence rates as the global approximation.

The projection-based interpolation $\Pi_{h,p}$ (of reference solution $\boldsymbol{u}_{ref}$), analyzed in [7], consists of three steps:

- evaluation of $\boldsymbol{u}_{ref}$ at mesh vertices and its extension to the element interior - resulting in (bi)linear vertex interpolant denoted by $\boldsymbol{u}_1$;
- projection of $\boldsymbol{u}_{ref} - \boldsymbol{u}_1$ in H_0^1 on edges and its extension to the element interior - resulting in edge interpolant denoted by $\boldsymbol{u}_2$: this step involves a discrete minimization problem (= solution of a system of linear equations) on each edge;
- projection of $\boldsymbol{u}_{ref} - \boldsymbol{u}_1 - \boldsymbol{u}_2$ on the element bubble functions; this step involves one solution of a system of linear equations for each element.

With a suitable projection-based interpolation in hand, one step of the mesh optimization looks as follows [8]:

1. Perform the global *hp*-refinement and compute fine mesh solution $\boldsymbol{u}_{h/2,p+1}$.

2. Compute elementwise error $||\boldsymbol{u}_{h/2,p+1} - \boldsymbol{u}_{h,p}||_{e,K}$ for all $T \in \mathcal{T}_{h,p}$.

3. Determine the element isotropy flags (= determine if the element is going to be refined isotropically or anisotropically).

4. Determine optimal refinement for each edge in the mesh $\mathcal{T}_{h,p}$ using competitive refinements.

5. Determine the maximum edge error decrease rate and identify all edges with error decrease equal at least to (e.g.) one third of the maximal one; those edges are going to be refined.

6. Use the information about edge *h*-refinements and the element isotropy flags to decide about *h*-refinements for all elements.

7. Determine optimal orders of approximation for all element interiors monitoring the error decrease rate.

8. Enforce the *minimum rule* to all edges in the mesh: order of approximation for an edge must be equal to the minimum of orders for the adjacent elements.

The fully automatic *hp*-adaptive strategy proposed in [8] starts with an initial mesh and repeats the mesh-optimization procedure until a sufficient accuracy of the solution (measured in the energy norm of the difference of $\boldsymbol{u}_{h/2,p+1} - \boldsymbol{u}_{h,p}$) is reached. Solution $\boldsymbol{u}_{h/2,p+1}$ can be used as a final result.

Let us mention that strategies based on the reference solution are not the only possibility – for an alternative strategy based on monitoring local *h*-convergence rates, see [1].

2 Fully automatic goal-oriented *hp*-adaptivity

We have given now enough background to introduce the goal-oriented *hp*-adaptive strategy. The basic difference between the energy driven *hp* adaptive strategy from [8], and the new approach, is that instead of minimizing the error in the energy norm (1.16), we will minimize the error in the quantity of interest,

$$|L(\boldsymbol{u}_{h/2,p+1}) - L(\boldsymbol{u}_{h,p})|. \tag{2.19}$$

Here $\boldsymbol{u}_{h/2,p+1}$ denotes the fine mesh solution corresponding to the globally refined current mesh, *both* in h and p.

Replacing the exact solution $\boldsymbol{u}$ and the (exact) dual solution $\boldsymbol{v}$ with the corresponding fine mesh solutions $\boldsymbol{u}_{h/2,p+1}, \boldsymbol{v}_{h/2,p+1}$, resp., we repeat now the steps discussed in subsection 1.2, to arrive at the following identity,

$$|L(\boldsymbol{u}_{h/2,p+1}) - L(\boldsymbol{u}_{h,p})| = b(\boldsymbol{u}_{h/2,p+1} - \boldsymbol{u}_{h,p}, \boldsymbol{v}_{h/2,p+1} - \boldsymbol{v}_{h,p}). \tag{2.20}$$

We assume that the bilinear form $b(\boldsymbol{u}, \boldsymbol{v})$ can be split into a bilinear, positive definite part $a(\boldsymbol{u}, \boldsymbol{v})$ and a compact perturbation $c(\boldsymbol{u}, \boldsymbol{v})$, see [9],

$$b(\boldsymbol{u}, \boldsymbol{v}) = a(\boldsymbol{u}, \boldsymbol{v}) + c(\boldsymbol{u}, \boldsymbol{v}). \tag{2.21}$$

Recall that in (2.20) $\boldsymbol{u}_{h/2,p+1}$ and $\boldsymbol{u}_{h,p}$ are fine and coarse grid solution to the original problem, $\boldsymbol{v}_{h/2,p+1}$ is the fine grid solution of the dual problem, and $\boldsymbol{v}_{h,p}$ stands for any coarse grid test function. We make now the following assumptions.

1. We select for $\boldsymbol{v}_{h,p}$ the projection-based interpolant of fine mesh dual problem solution,

$$\begin{aligned} L(\boldsymbol{u}_{h/2,p+1}) - L(\boldsymbol{u}_{h,p}) = b(\boldsymbol{u}_{h/2,p+1} - \Pi \boldsymbol{u}_{h/2,p+1}, \boldsymbol{v}_{h/2,p+1} - \Pi \boldsymbol{v}_{h/2,p+1}) \\ -b(\Pi \boldsymbol{u}_{h/2,p+1} - \boldsymbol{u}_{h,p}, \boldsymbol{v}_{h/2,p+1} - \Pi \boldsymbol{v}_{h/2,p+1}). \end{aligned} \tag{2.22}$$

2. We neglect the second term corresponding to the contribution of the difference between the coarse grid interpolant $\Pi \boldsymbol{u}_{h/2,p+1}$ and coarse grid solution.

   This leads to the estimate

$$\begin{aligned} |L(\boldsymbol{u}_{h/2,p+1}) - L(\boldsymbol{u}_{h,p})| &\leq \sum_{K \in \mathcal{T}_{h,p}} |b_K(\boldsymbol{u}_{h/2,p+1} - \Pi \boldsymbol{u}_{h/2,p+1}, \boldsymbol{v}_{h/2,p+1} - \Pi \boldsymbol{v}_{h/2,p+1})| \\ &\leq \sum_K \Big\{ |a_K(\boldsymbol{u}_{h/2,p+1} - \Pi \boldsymbol{u}_{h/2,p+1}, \boldsymbol{v}_{h/2,p+1} - \Pi \boldsymbol{v}_{h/2,p+1})| \\ &\quad + |\, c_K(\boldsymbol{u}_{h/2,p+1} - \Pi \boldsymbol{u}_{h/2,p+1}, \boldsymbol{v}_{h/2,p+1} - \Pi \boldsymbol{v}_{h/2,p+1})| \Big\} \\ &\leq \sum_K (1 + M_K) \|\boldsymbol{u}_{h/2,p+1} - \Pi \boldsymbol{u}_{h/2,p+1}\|_{e,K} \|\boldsymbol{v}_{h/2,p+1} - \Pi \boldsymbol{v}_{h/2,p+1}\|_{e,K}. \end{aligned} \tag{2.23}$$

   Here b_K, a_K, c_K denote element contributions to global forms b, a, c respectively and M_K stands for the continuity constant of bilinear form c_K,

$$\begin{aligned} |c_K(\boldsymbol{u}_{h/2,p+1} - \Pi \boldsymbol{u}_{h/2,p+1}, \boldsymbol{v}_{h/2,p+1} - \Pi \boldsymbol{v}_{h/2,p+1})| \\ \leq M_K \|\boldsymbol{u}_{h/2,p+1} - \Pi \boldsymbol{u}_{h/2,p+1}\|_{e,K} \|\boldsymbol{v}_{h/2,p+1} - \Pi \boldsymbol{v}_{h/2,p+1}\|_{e,K}. \end{aligned} \tag{2.24}$$

3. We expect constant M_K to be asymptotically (both in h and p) converging to zero, and we shall neglect it in our estimate.

This leads to the final estimate,

$$|L(\boldsymbol{u}_{h/2,p+1}) - L(\boldsymbol{u}_{h,p})| \leq \sum_{K \in \mathcal{T}_{h,p}} \|\boldsymbol{u}_{ref} - \Pi_{h,p}\boldsymbol{u}_{ref}\|_{e,K} \|\boldsymbol{v}_{ref} - \Pi_{h,p}\boldsymbol{v}_{ref}\|_{e,K} \, , \tag{2.25}$$

which is approximate in sense of neglecting the difference between fine mesh solution and fine mesh solution interpolant in (2.22). Consequently, instead of minimizing the projection based interpolation error,

$$\|\boldsymbol{u}_{h/2,p+1} - \Pi_{h,p}\boldsymbol{u}_{h/2,p+1}\|^2 = \sum_K \|\boldsymbol{u}_{h/2,p+1} - \Pi_{h,p}\boldsymbol{u}_{h/2,p+1}\|^2_{e,K} \, , \tag{2.26}$$

we shall modify the original *hp* strategy to minimize now estimate (2.25). The steps of the algorithm are analogous to those discussed in section 1.4.

1. Compute element contributions to estimate (2.25),

$$\|\boldsymbol{u}_{h/2,p+1} - \Pi_{h,p}\boldsymbol{u}_{h/2,p+1}\|_{e,K} \|\boldsymbol{v}_{h/2,p+1} - \Pi_{h,p}\boldsymbol{v}_{h/2,p+1}\|_{e,K}, \tag{2.27}$$

   for all $T \in \mathcal{T}_{h,p}$.

2. Determine the element isotropy flags. An element is declared to be a candidate for an anisotropic refinement if *both* differences $\boldsymbol{u}_{h/2,p+1} - \boldsymbol{u}_{h,p}$ and $\boldsymbol{v}_{h/2,p+1} - \boldsymbol{v}_{h,p}$ represent the same anisotropic behavior.

3. Determine optimal refinement for each edge e in the current mesh $\mathcal{T}_{h,p}$ comparing competitive refinements. Use product of the interpolation errors for the primal and dual problems in place of the interpolation error of the fine mesh solution,

$$\|\boldsymbol{u}_{h/2,p+1} - \Pi_{h,p}\boldsymbol{u}_{h/2,p+1}\|_{H^{\frac{1}{2}}_{00}(e)} \|\boldsymbol{v}_{h/2,p+1} - \Pi_{h,p}\boldsymbol{v}_{h/2,p+1}\|_{H^{\frac{1}{2}}_{00}(e)} \, . \tag{2.28}$$

4. Determine the maximum edge error decrease rate and identify all edges with error decrease greater or equal than one third of the maximal one; those edges are going to be refined.

5. Use the information about edge h-refinements and the element isotropy flags to decide about h-refinements for all elements.

6. Determine optimal orders of approximation for all element interiors monitoring the decrease rate of the product of the element interpolation errors (2.27).

7. Enforce the *minimum rule* for all edges in the mesh: order of approximation for an edge must be equal to the minimum of orders for the adjacent elements.

With the one step minimization strategy described above, the ultimate goal-oriented *hp* strategy looks as follows.

1. Initiate $k := 0$.
2. Consider mesh $\mathcal{T}_{h,p}^k$ and corresponding space of functions $V_{h,p}^k$.
3. Solve direct problem on the coarse mesh: $b(\boldsymbol{u}_{h,p}^k, \boldsymbol{v}) = f(\boldsymbol{v})$, for all $\boldsymbol{v} \in V_{h,p}^k$.
4. Solve dual problem on the coarse mesh: $b(\boldsymbol{u}, \boldsymbol{v}_{h,p}^k) = L(\boldsymbol{u})$, for all $\boldsymbol{u} \in V_{h,p}^k$.
5. Construct globally *hp*-refined mesh $\mathcal{T}_{h/2,p+1}^k$ and the corresponding finite element space $V_{h/2,p+1}^k$.
6. Solve direct problem on the fine mesh: $b(\boldsymbol{u}_{h/2,p+1}^k, \boldsymbol{v}) = f(\boldsymbol{v})$, for all $\boldsymbol{v} \in V_{h/2,p+1}^k$.
7. Solve dual problem on the fine mesh: $b(\boldsymbol{u}, \boldsymbol{v}_{h/2,p+1}^k) = L(\boldsymbol{u})$, for all $\boldsymbol{u} \in V_{h/2,p+1}^k$.
8. Compute estimate (2.25). If the estimated difference (relative to fine mesh goal $L(\boldsymbol{u}_{h/2,p+1})$ is within the prescribed tollerance, quit.
9. Apply the mesh optimization procedure described above to construct next optimal mesh $\mathcal{T}_{h,p}^{k+1}$.

Remarks:

1. Similarly as in [8], we replace the $H_{00}^{\frac{1}{2}}(e)$ norm with a weighted $H_0^1(e)$ norm, see [8] for details.
2. Notice that the stopping criterion is based on the actual difference of the fine and coarse mesh goals and not its estimate.

Energy and goal driven *h*-adaptivity

One of the goals of the presented work is to gain some experience with how much can we gain using *hp*-adaptivity when compared with *h*-adaptivity only using quadratic elements. The choice of quadratic elements seems to be fair as, in general, they deliver vastly superior results to linear elements, and their implementation is much simpler than, say, cubic elements. Quadratic element, for instance, have only one d.o.f. (scalar case) per edge, face, and element interior (no orientation needed !) and present a good balance between accuracy and complexity of the corresponding implementation.

There are many possible *h*-adaptive schemes, for both energy and goal-driven adaptivity, and we present now shortly the two schemes that we have used for our comparison. We shall discuss one step for both of the algorithms only.

Energy driven h-adaptive algorithm

Given a coarse mesh τ_h^k and corresponding finite element space V_h^k, we construct the next coarse mesh τ_h^{k+1} as follows.

1. Solve direct problem on the coarse mesh: $b(\boldsymbol{u}_h^k, \boldsymbol{v}) = f(\boldsymbol{v})$, for all $\boldsymbol{v} \in V_h^k$.
2. Construct globally h-refined mesh $\tau_{h/2}^k$ and the corresponding FE space $V_{h/2}^k$.
3. Solve direct problem on the fine mesh: $b(\boldsymbol{u}_{h/2}^k, \boldsymbol{v}) = f(\boldsymbol{v})$, for all $\boldsymbol{v} \in V_{h/2}^k$.
4. Compute the difference between the coarse and fine mesh solutions,

$$\|\boldsymbol{u}_{h/2}^k - \boldsymbol{u}_h^k\|_e^2 = \sum_{K \in \tau_h^k} \|\boldsymbol{u}_{h/2}^k - \boldsymbol{u}_h^k\|_{e,K}^2 \ .$$

   When computing the element contributions, determine the anisotropy flags for the elements.
5. Quit if the error estimate is below the prescribed tollerance.
6. Determine the maximum element contribution to the error estimate, and refine all elements that contribute with error within one third of the maximum one. Use the isotropy flags to decide between the isotropic and anisotropic refinements.

Goal driven h-adaptive algorithm

Given a coarse mesh τ_h^k and corresponding finite element space V_h^k, we construct the next coarse mesh τ_h^{k+1} as follows.

1. Solve direct problem on the coarse mesh: $b(\boldsymbol{u}_h^k, \boldsymbol{v}) = f(\boldsymbol{v})$, for all $\boldsymbol{v} \in V_h^k$.
2. Solve dual problem on the coarse mesh: $b(\boldsymbol{u}, \boldsymbol{v}_h^k) = L(\boldsymbol{u})$, for all $\boldsymbol{u} \in V_h^k$.
3. Construct globally h-refined mesh $\tau_{h/2}^k$ and the corresponding FE space $V_{h/2}^k$.
4. Solve direct problem on the fine mesh: $b(\boldsymbol{u}_{h/2}^k, \boldsymbol{v}) = f(\boldsymbol{v})$, for all $\boldsymbol{v} \in V_{h/2}^k$.
5. Solve dual problem on the fine mesh: $b(\boldsymbol{u}, \boldsymbol{v}_{h/2}^k) = L(\boldsymbol{u})$, for all $\boldsymbol{u} \in V_{h/2}^k$.
6. Compute the estimate of the difference in goal for the coarse and fine mesh solutions,

$$|L(\boldsymbol{u}_{h/2}^k) - L(\boldsymbol{u}_h^k)| \stackrel{\sim}{<} \sum_{K \in \tau_h^k} \|\boldsymbol{u}_{h/2}^k - \boldsymbol{u}_h^k\|_{e,K} \|\boldsymbol{v}_{h/2}^k - \boldsymbol{v}_h^k\|_{e,K} \ .$$

   When computing the element contributions, determine the anisotropy flags for the elements.

7. Quit if the difference in goals for the fine and coarse mesh solutions is below the prescribed tollerance.

8. Determine the maximum element contribution to the error estimate, and refine all elements that contribute with error within one third of the maximum one. Use the isotropy flags to decide between the isotropic and anisotropic refinements.

3 Model problem

We consider the standard L-shape Ω domain problem, see [8].

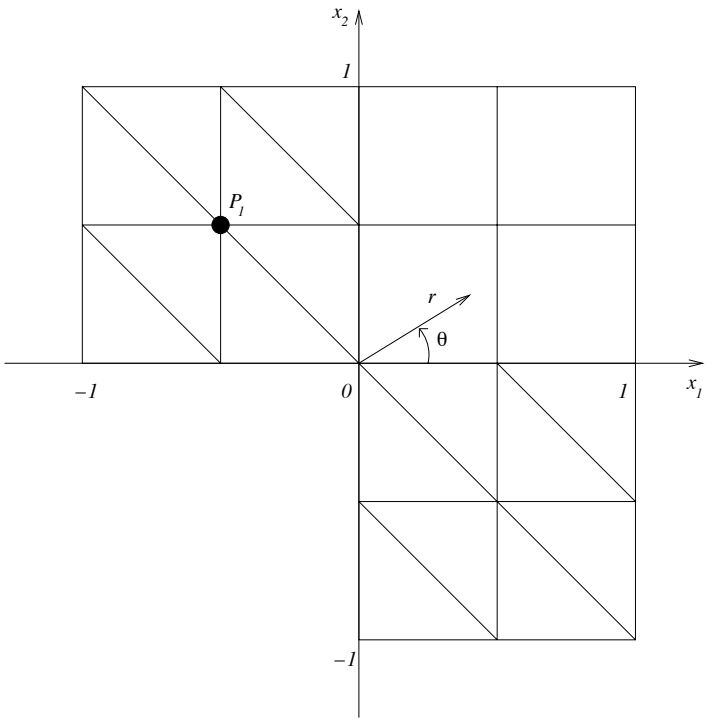

Figure 2: Geometry and initial mesh.

We solve the Laplace equation

$$-\triangle u = 0 \tag{3.29}$$

in Ω, with Dirichlet boundary conditions $u(x) = \varphi(x)$ for all $x \in \partial\Omega$. Function φ is chosen to be compatible with the harmonic function

$$u(x_1, x_2) = r^{2/3} \sin(2\theta/3 + \pi/3) \tag{3.30}$$

where (r, z) are standard polar coordinates. Derivatives of the solution are singular at origin $[0, 0]$.

The goal of our computation is the average value of the solution u over a small neighborhood Ω_s of point $P_1 = [-0.5, 0.5]$ (shown in Fig. 2).

Figures 3, 4, 5, 6 show meshes which have been obtained to yield a relative error in the quantity of interest to be less than 10^{-5}. Scale on the right hand side indicates the order of polynomial approximation, starting with $p = 1$.

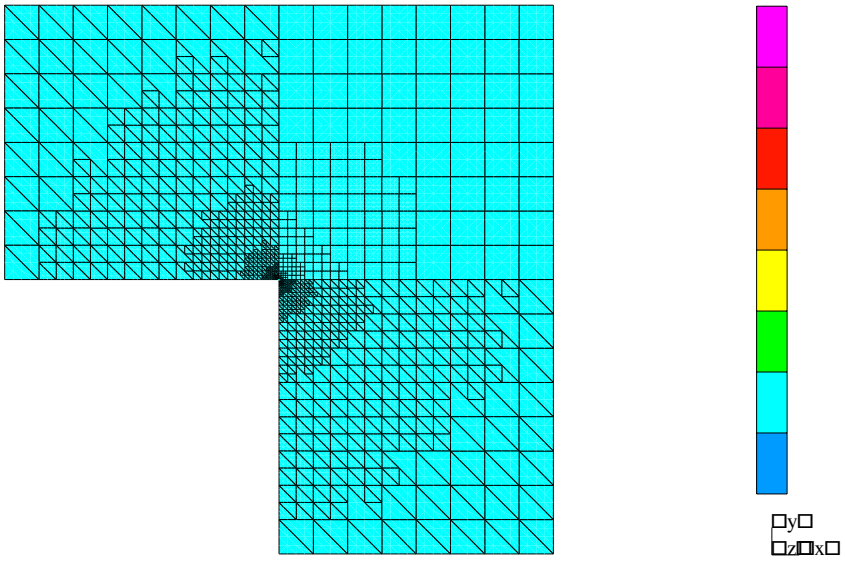

Figure 3: Energy-based h-adaptivity. Mesh after 18 h-refinements (all elements are second-order), number of DOF = 3114.

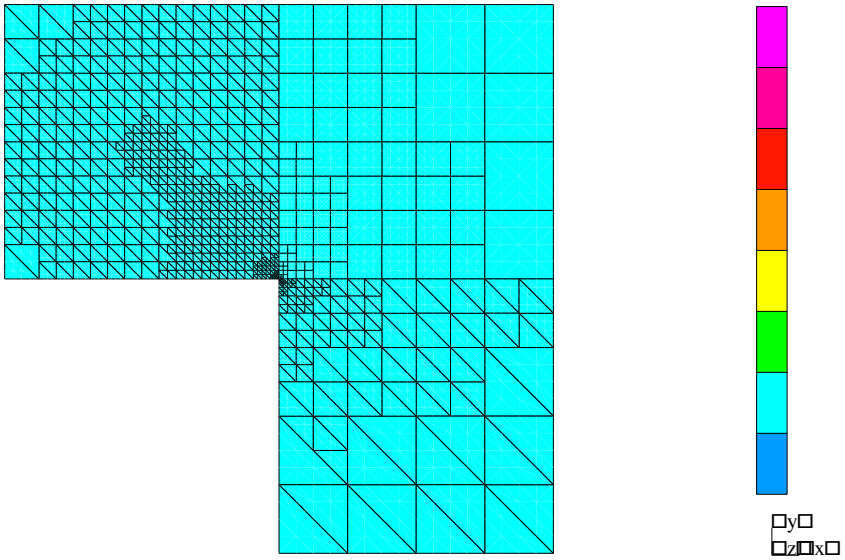

Figure 4: Goal-oriented h-adaptivity. Mesh after 17 h-refinements (all elements are second-order), number of DOF = 2448.

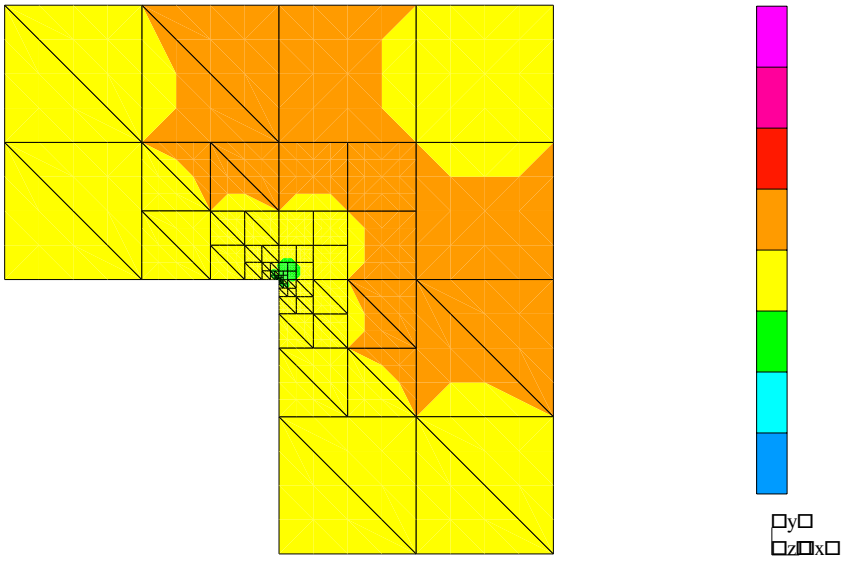

Figure 5: Energy-based *hp*-adaptivity. Mesh after 15 *hp*-refinements, number of DOF = 1366.

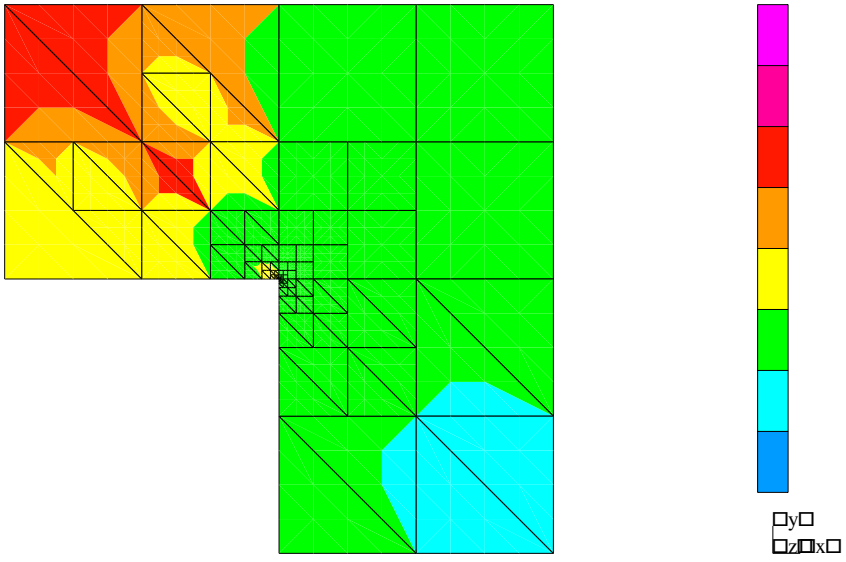

Figure 6: Goal-oriented *hp*-adaptivity. Mesh after 10 *hp*-refinements, number of DOF = 803.

The neighborhood Ω_s of point $P_1 = [-0.5, 0.5]$ is defined as follows: tet us consider the mesh edges e_j, $j = 1, 2, \ldots, 6$, starting at P_1. For each of them we consider a point Q_j which lies at e_j and whose distance from P_1 is

$$|Q_j - P_1| = \frac{|e_j|}{2^5}. \tag{3.31}$$

The neighborhood Ω_s is defined as the convex envelope of points $Q_1, Q_2, \ldots, Q_6$. We mention that the choice of the shape of neighborhood Ω_s has been motivated with the ease of numerical integration over Ω_s only.

Fig. 7 shows the history of the relative error in goal for all four tested approaches. The x-axis represents the number of degrees of freedom.

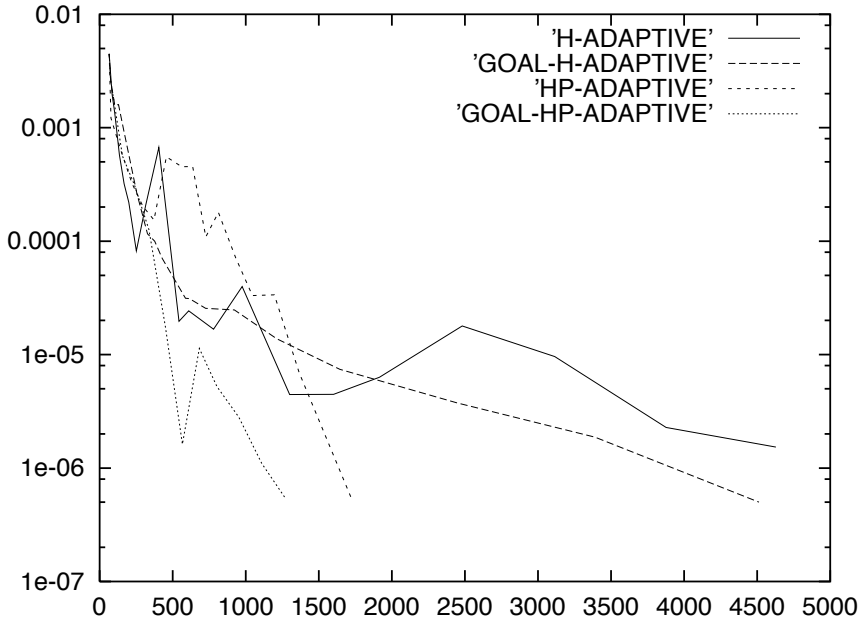

Figure 7: Relative error wrt. the exact solution in goal.

4 The radiation problem (continued)

Finally we return to the motivating problem introduced in paragraph 1.1. We have to control the error in the nonlinear quantity $N(E)$, i.e. to find an approximation $E_{h,p}$ of E such that

$$|N(E_{h,p}) - N(E)| \leq TOL \tag{4.32}$$

where E is the (unknown) exact solution.

Dual problem:

We look for a suitable linear functional of interest for the dual problem approximating $N(E)$. Assuming that the value

$$\int_{B(P_1,r_c)} E_{h,p}\,\mathrm{d}r\mathrm{d}z \tag{4.33}$$

corresponding to the approximate solution will lie close to

$$\int_{B(P_1,r_c)} E\,\mathrm{d}r\mathrm{d}z, \tag{4.34}$$

gives us the right to approximate

$$|N(E_{h,p}) - N(E)| = 20\left|\log_{10}\frac{\int_{B(P_1,r_c)} E_{h,p}\,\mathrm{d}r\mathrm{d}z}{\int_{B(P_1,r_c)} E\,\mathrm{d}r\mathrm{d}z}\right| \approx \frac{20}{\ln 10}\left|\frac{\int_{B(P_1,r_c)} E_{h,p}\,\mathrm{d}r\mathrm{d}z - \int_{B(P_1,r_c)} E\,\mathrm{d}r\mathrm{d}z}{\int_{B(P_1,r_c)} E\,\mathrm{d}r\mathrm{d}z}\right|. \tag{4.35}$$

We see that due to the 'linearity' of function $\log_{10}(y)$ at $y = 1$, the minimization of the error in $N(E)$ translates into the minimization of the error in the quantity

$$L(E) = \int_{B(P_1,r_c)} E\,\mathrm{d}r\mathrm{d}z. \tag{4.36}$$

Thus, the goal of our computation is the integral of E over the receiving antenna $B(P_1, r_c)$. The constant $20/\ln(10)$ will play a role only in the stopping criterion for the adaptive algorithm.

4.1 Results

In this paragraph we show a few results (sequences of meshes) of energy-based and goal-oriented h- and hp-adaptive schemes, applied to the radiation problem. All schemes start from the same coarse initial mesh consisting of second-order elements.

4.1.1 Energy-based and goal-oriented h-adaptivity

Similarly as in Section 3, the scale on the righ hand side represents the order of polynomial approximation. Energy-based and goal-oriented h-adaptivity will be performed using second order elements only,

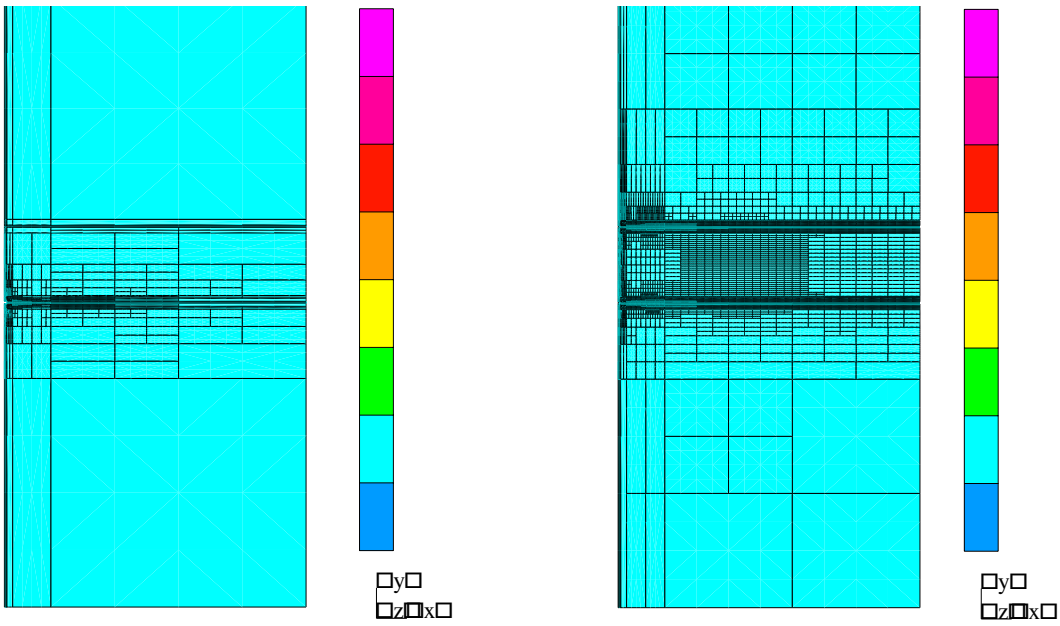

Figure 8: Energy-based h-adaptivity (left) and goal-oriented h-adaptivity (right), meshes corresponding to approx. 11000 degrees of freedom.

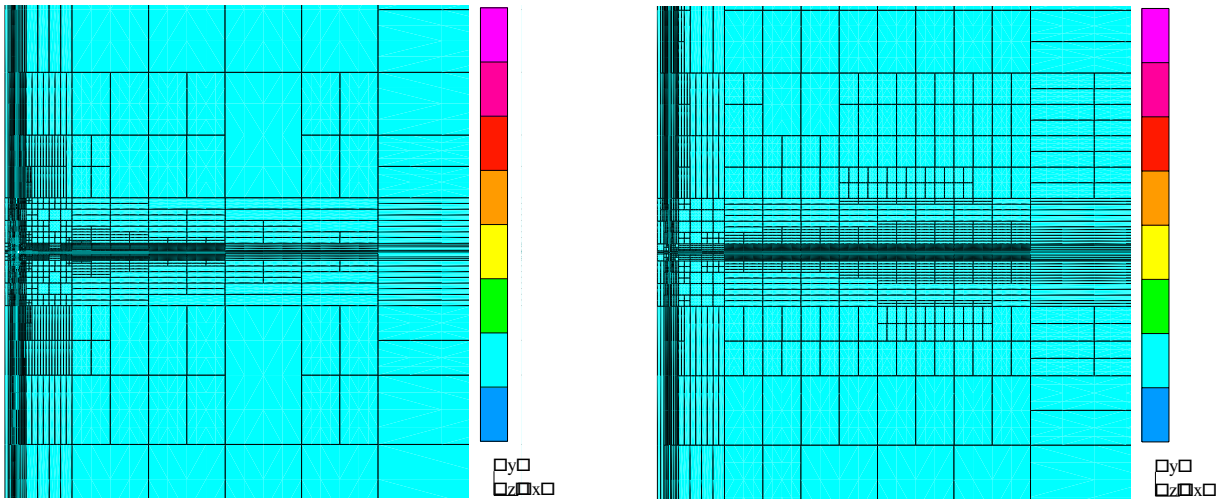

Figure 9: Energy-based h-adaptivity (left) and goal-oriented h-adaptivity (right), zoom = 10 towards the emitting antenna.

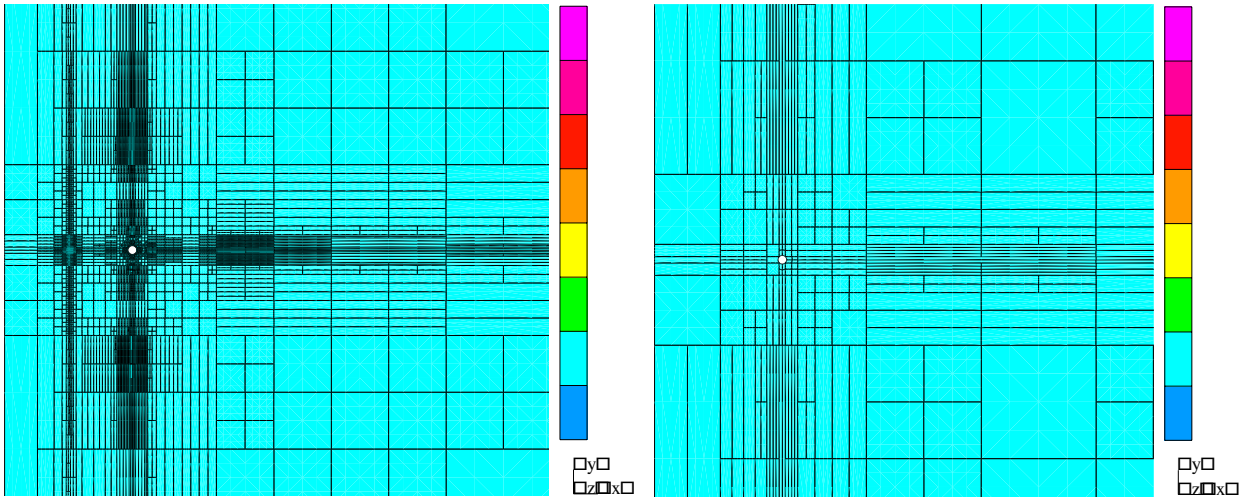

Figure 10: Energy-based h-adaptivity (left) and goal-oriented h-adaptivity (right), zoom = 100 towards the emitting antenna.

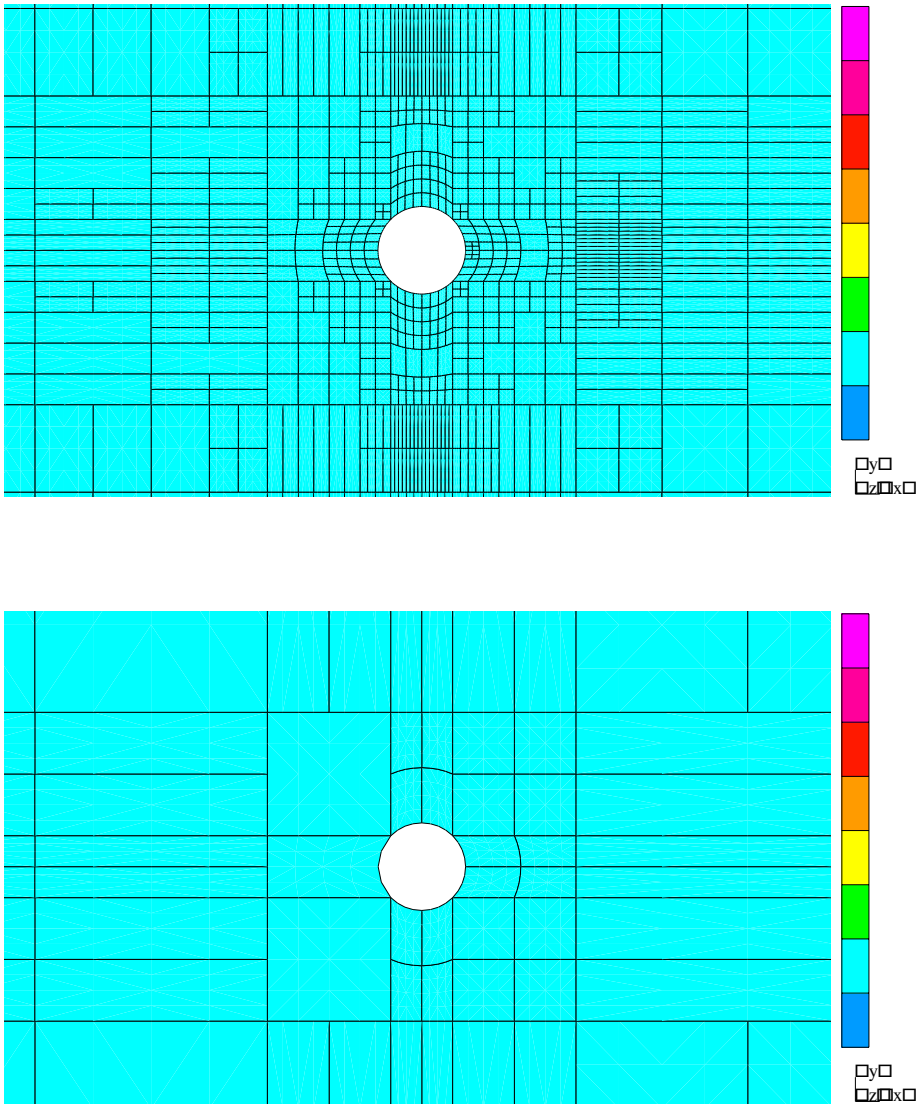

Figure 11: Energy-based h-adaptivity (above) and goal-oriented h-adaptivity (below), zoom = 1000 towards the emitting antenna.

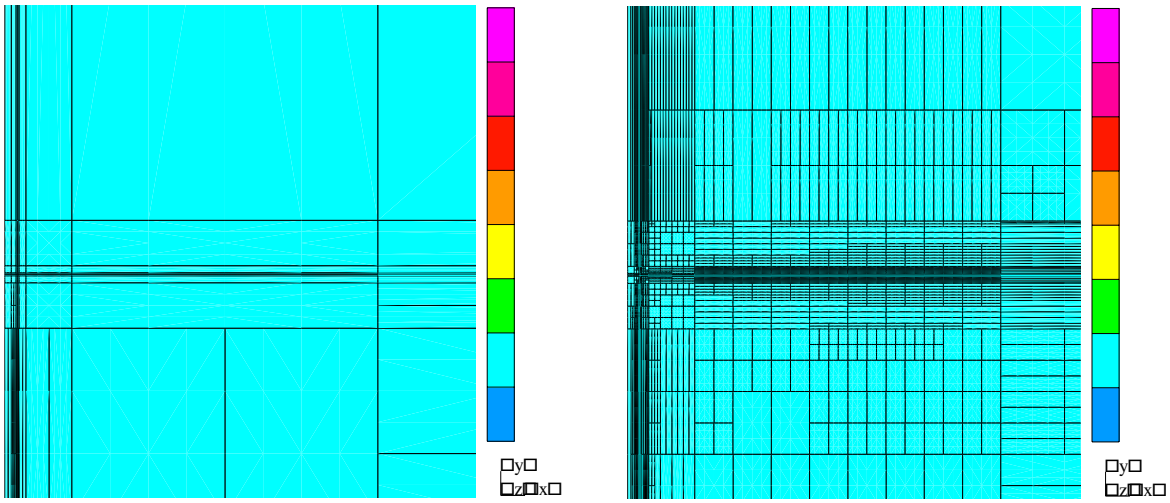

Figure 12: Energy-based h-adaptivity (left) and goal-oriented h-adaptivity (right), zoom = 10 towards the receiving antenna.

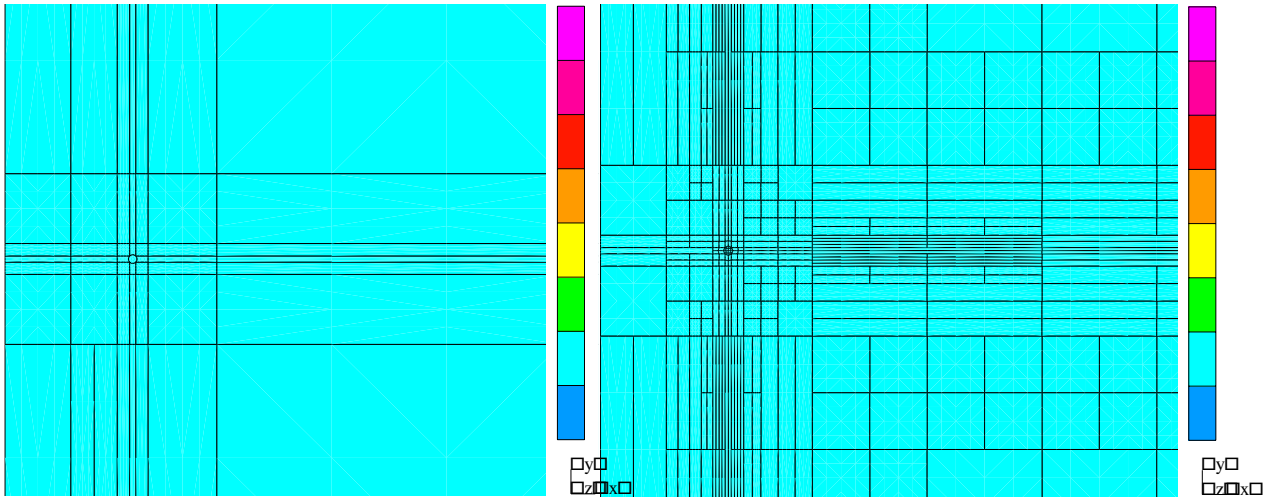

Figure 13: Energy-based h-adaptivity (left) and goal-oriented h-adaptivity (right), zoom = 100 towards the receiving antenna.

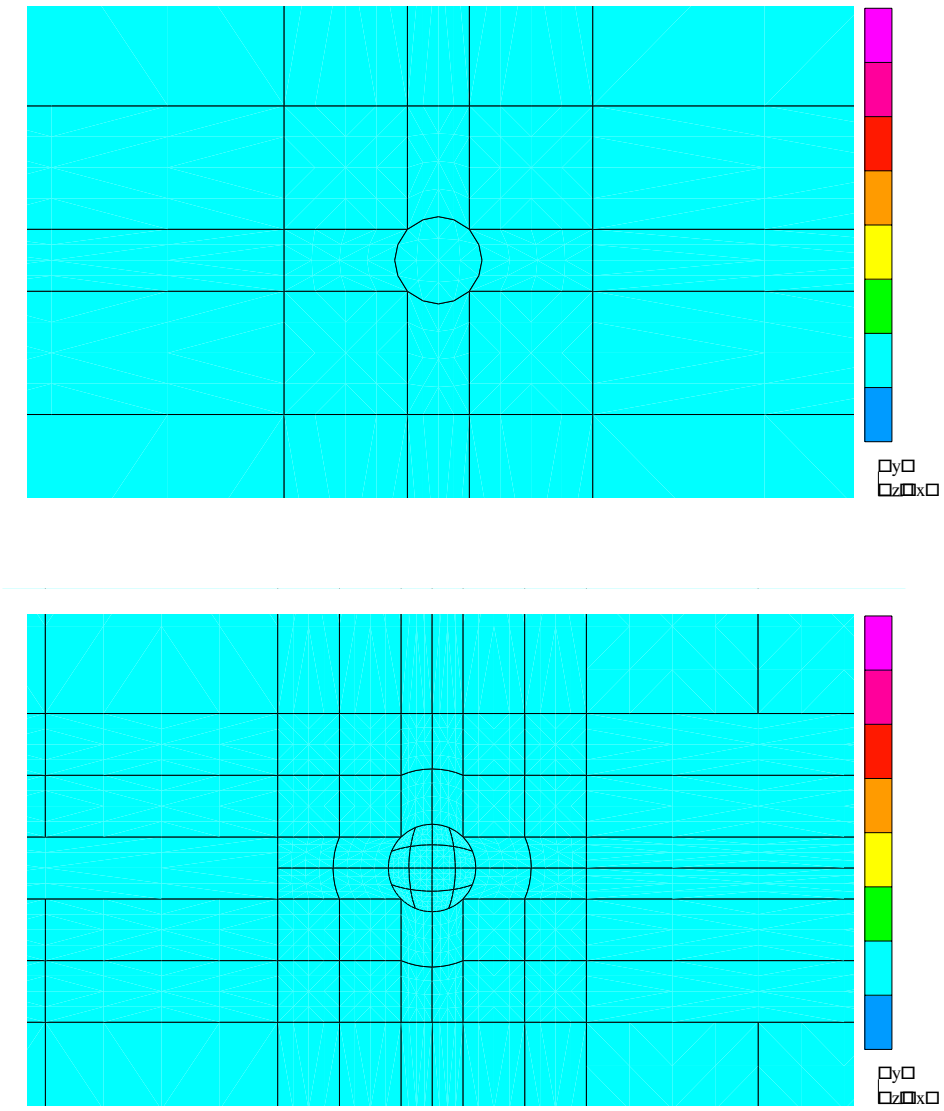

Figure 14: Energy-based h-adaptivity (above) and goal-oriented h-adaptivity (below), zoom = 1000 towards the receiving antenna.

4.1.2 Energy-based and goal-oriented *hp*-adaptivity

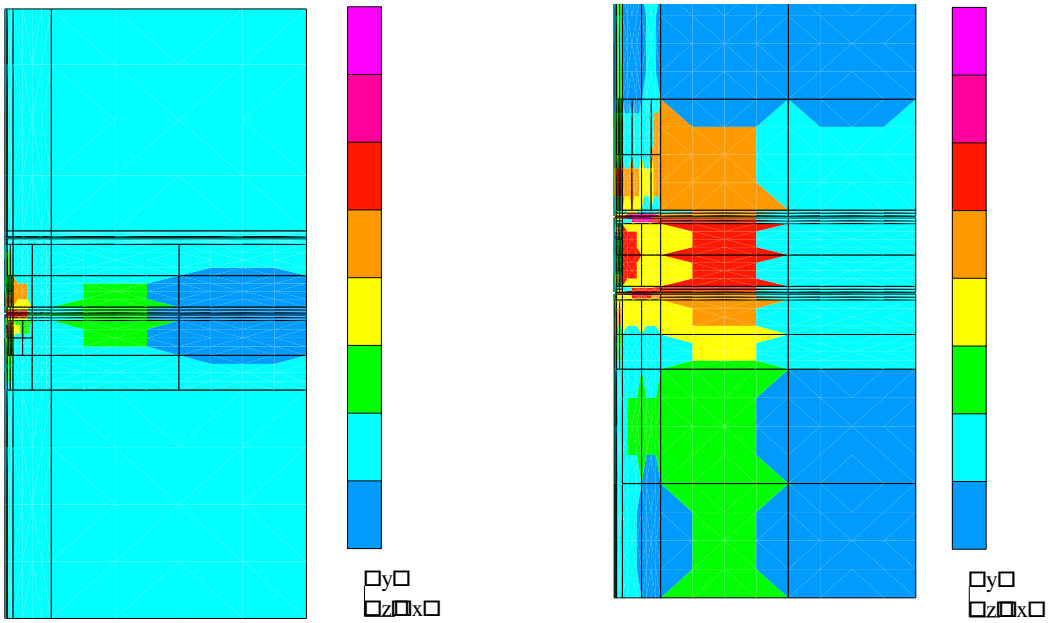

Figure 15: Energy-based *hp*-adaptivity (left) and goal-oriented *hp*-adaptivity (right), meshes corresponding to approx. 11000 degrees of freedom.

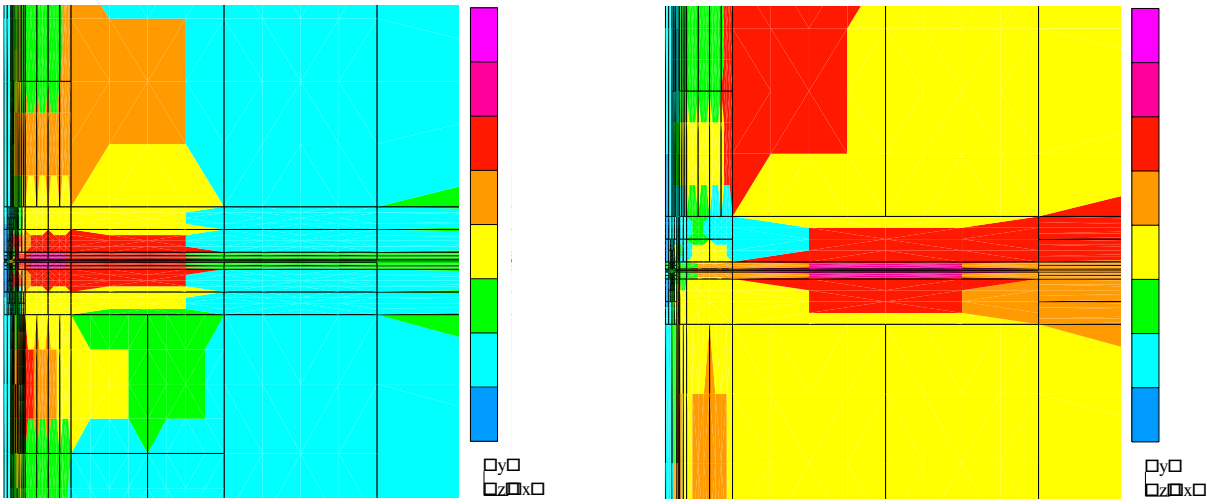

Figure 16: Energy-based *hp*-adaptivity (left) and goal-oriented *hp*-adaptivity (right), zoom = 10 towards the emitting antenna.

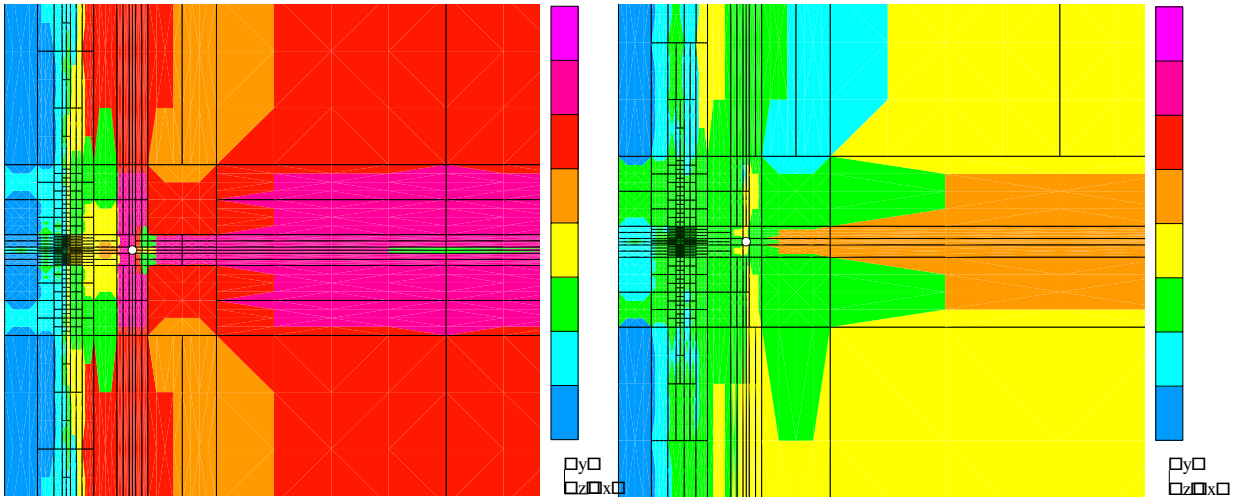

Figure 17: Energy-based *hp*-adaptivity (left) and goal-oriented *hp*-adaptivity (right), zoom = 100 towards the emitting antenna.

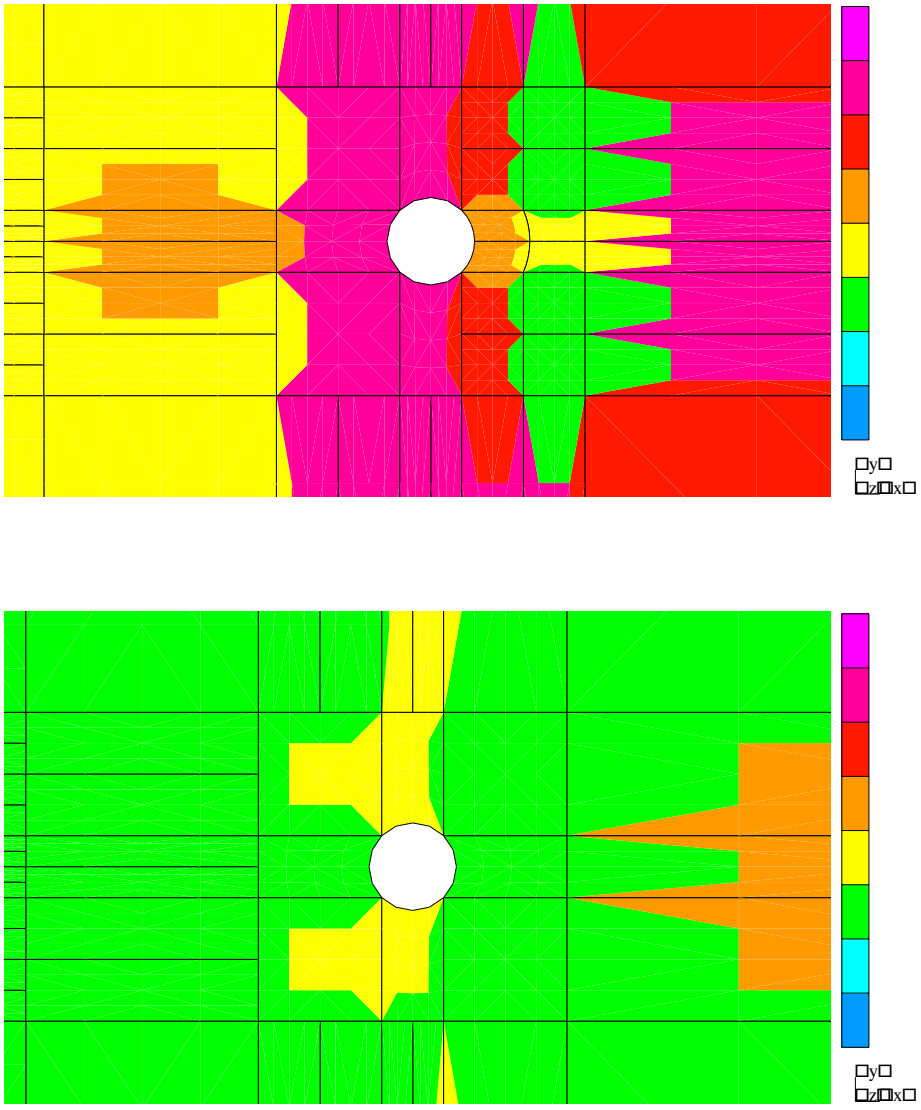

Figure 18: Energy-based *hp*-adaptivity (above) and goal-oriented *hp*-adaptivity (below), zoom = 1000 towards the emitting antenna.

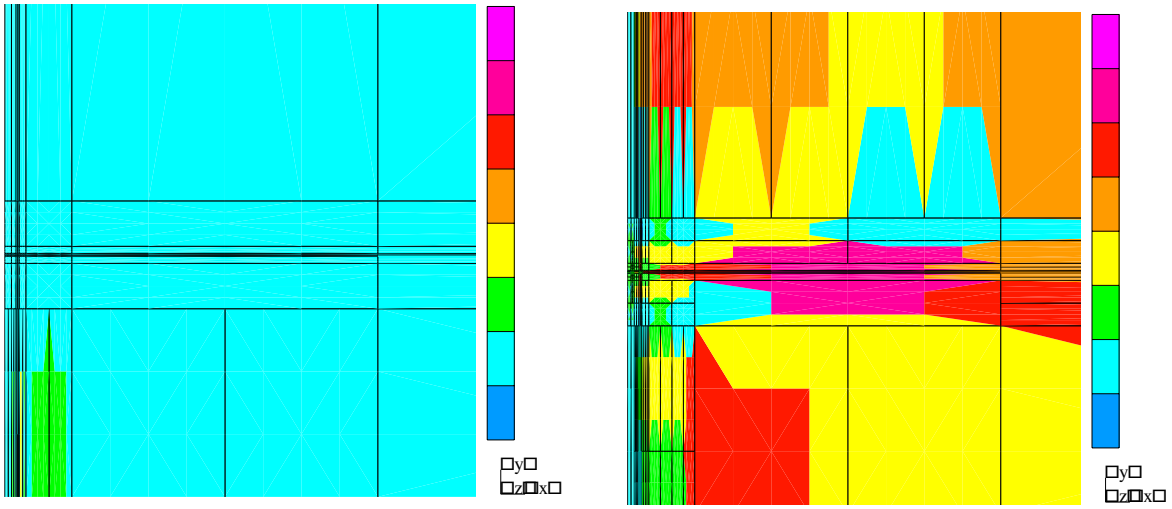

Figure 19: Energy-based *hp*-adaptivity (left) and goal-oriented *hp*-adaptivity (right), zoom = 10 towards the receiving antenna.

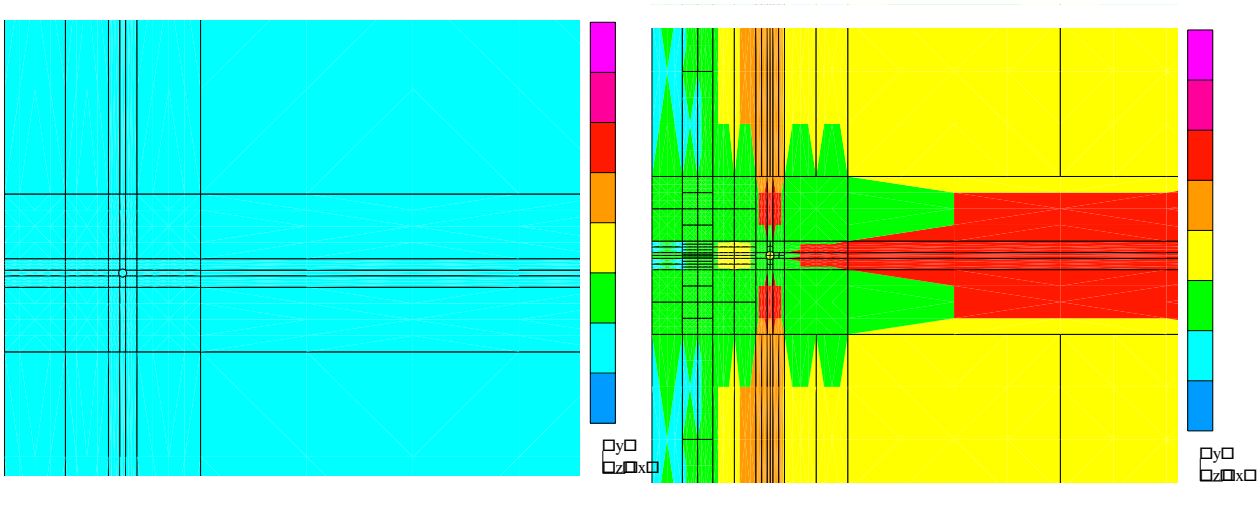

Figure 20: Energy-based *hp*-adaptivity (left) and goal-oriented *hp*-adaptivity (right), zoom = 100 towards the receiving antenna.

Fig. 22 shows the history of the relative error in goal (i.e. in the nonlinear quantity (1.6)) for all four tested approaches. The unknown exact solution to the radiation problem is replaced by the corresponding fine mesh solution for the error evaluation. The x-axis represents the number of degrees of freedom.

The presented results show a dramatic difference between the energy and goal driven adaptivity. The corresponding meshes are essentially different, and the goal-oriented adaptivity delivers results that are at least an order of magnitude better.

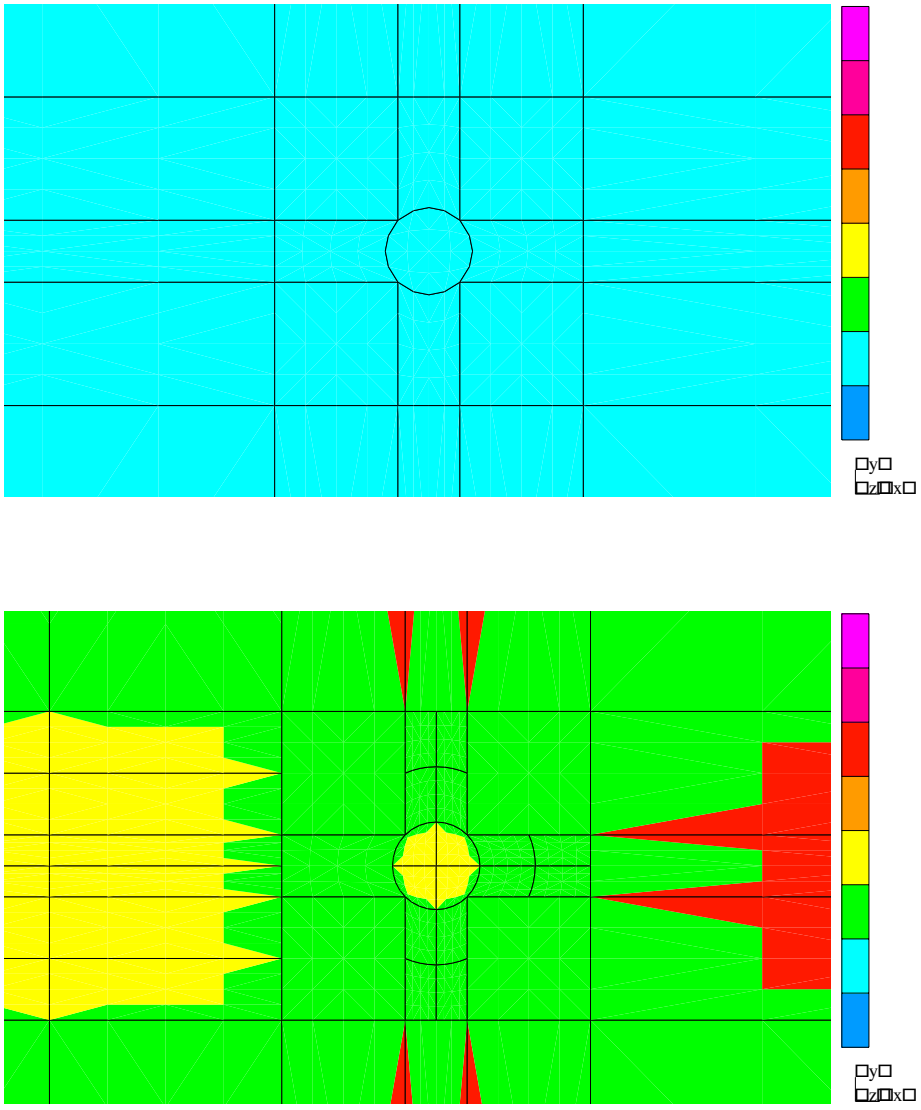

Figure 21: Energy-based *hp*-adaptivity (above) and goal-oriented *hp*-adaptivity (below), zoom = 1000 towards the receiving antenna.

Concerning the difference between the goal-driven *h*- and *hp*-adaptive schemes, we can risk a statement that, within the investigated range of problem size, *hp*-adaptivity delivers results that are an order of magnitude better than those produced by *h*-adaptivity only.

For all investigated strategies, the (estimated or computed) error in goal does not decrease monotonically, especially for energy driven schemes.

Finally, we would like to emphasize that for the antenna problem, that has motivated this research project, the goal oriented *hp*-adaptive scheme has delivered an outstanding 1/10 of a percent accuracy (on the decibel scale) which seems to be more than satisfactory from the

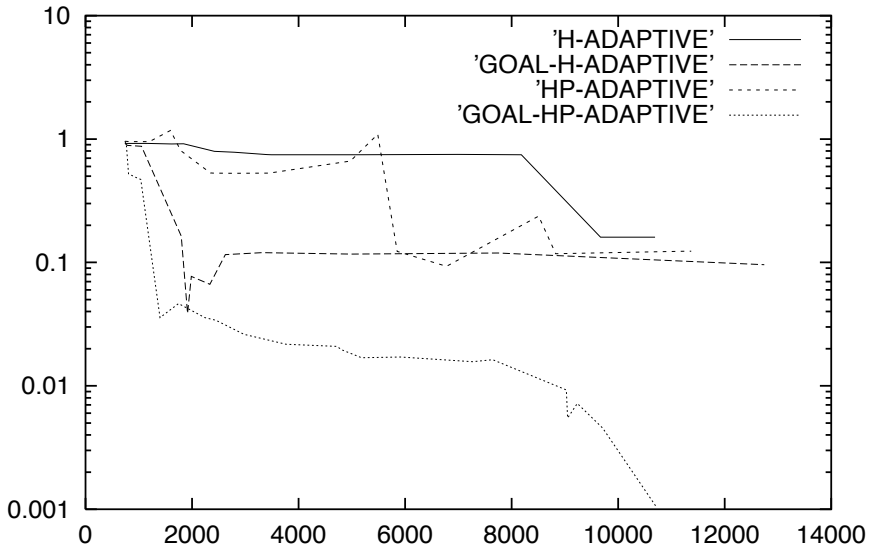

Figure 22: Relative error in goal (h-adaptivity with quadratic elements only, hp-adaptivity with initially quadratic elements).

practical point of view.

5 Conclusions

The aim of this study was to bring together the advantages of two powerful tools of numerical mathematics, the hp-adaptivity and the goal-oriented adaptivity, into a fully automatic goal-oriented hp-adaptive strategy for elliptic problems. We have extended an existing fully automatic hp-adaptive strategy in energy norm by introducing the solution of the dual problem and applying it to the mesh optimization algorithm based on the minimization of the projection-based hp-interpolation error of reference solutions to both the direct and the dual problems.

The numerical results presented in the last two sections demonstrate the advantages of this approach with respect to both the goal-oriented h-adaptive strategy and hp-adaptive strategy in energy norm.

However, as almost with all 2D computations, also this work is merely a proof of concept. The ultimate challenge we are heading for is the fully automatic goal-oriented hp-adaptivity in three spatial dimensions, on which we hope to report soon.

References

[1] M. Ainsworth, B. Senior, "Aspects of an *hp*-adaptive Finite Element Method: Adaptive Strategy, Conforming Approximation and Efficient Solvers", *Technical Report No. 1997/2*, Department of Mathematics and Computer Science, University of Leicester, England.

[2] I. Babuška, T. Strouboulis, K. Copps, S. K. Gangaraj, and C. S. Upadhyay, "A-Posteriori Error Estimation for Finite Element and Generalized Finite Element Method", *TICAM Report 98-01*, The University of Texas at Austin, 1998.

[3] R. Becker and R. Rannacher, "Weighted A-Posteriori Error Control in FE Method", *ENUMATH-95, Paris*, Sept. 1995.

[4] R. Becker and R. Rannacher, "A Feedback Approach to Error Control in Finite Elements Methods: Basic Analysis and Examples", *East-West J. Numer. Math.* **4**, 237-264, 1996.

[5] F. Cirak and E. Ramm, "A-Posteriori Error Estimation and Adaptivity for Linear Elasticity Using the Reciprocal Theorem", *Comp. Meth. in Appl. Mech. and Eng.* **156**, 351-362, 1998.

[6] L. Demkowicz, J.T.Oden, W.Rachowicz, O. Hardy, "Toward a Universal *hp*-Adaptive Finite Element Strategy. Part 1: Constrained Approximation and Data Structure", *Comput. Methods Appl. Math. Engrg.* **77**, 79-112, 1989.

[7] L. Demkowicz, and I. Babuška, "Optimal p Interpolation Error Estimates for Edge Finite Elements of Variable Order in 2D", *TICAM Report 01-11*, submitted to *SIAM Journal on Numerical Analysis*.

[8] L. Demkowicz, W. Rachowicz, and Ph. Devloo, "A Fully Automatic hp-Adaptivity", *Journal of Scientific Computing* **17**, Nos.1-3, 127-155, 2002.

[9] L. Demkowicz, "Asymptotic Convergence in Finite and Boundary Element Methods: Part 1: Theoretical Results", *Computers Math. Applic.* **27**, No. 12, 69-84, 1994.

[10] J. R. Lovell, *Finite Element Methods in Resistivity Logging*, Delft University of Technology, 38-45, 1993.

[11] J.T.Oden, L. Demkowicz, W.Rachowicz, T.A.Westermann, "A-Posteriori Error Analysis in Finite Elements. The Element Residual Methods for Symmetrizable Problems With Applications to Compressible Euler and Navier-Stokes Equations", *Comput. Methods Appl. Math. Engrg.* **82**, 183-203, 1990.

[12] J. T. Oden, S. Prudhomme, "Goal-Oriented Error Estimation and Adaptivity for the Finite Element Method" *Comp. Math. Appl.* **41**, 735-756, 2001.

[13] M. Paraschivoiu and A. T. Patera, "A Hierarchical Duality Approach to Bounds for the Outputs of Partial Differential Equations", *Comp. Meth. in Appl. Mech. and Eng.* **158**, 389-407, 1998.

[14] J. Peraire and A. T. Patera, "Bounds for Linear-Functional Outputs of Coercive Partial Differential Equations: Local Indicators and Adaptive Refinement", In P. Ladevèze and J. T. Oden, editors, *Advances in Adaptive Computational Methods in Mechanics*, 199-215. Elsevier, Amsterdam, 1998.

[15] W.Rachowicz, J.T.Oden, L. Demkowicz, "Toward a Universal *hp*-Adaptive Finite Element Strategy. Part 3: Design of *hp* Meshes", *Comput. Methods Appl. Math. Engrg.* **77**, No. 2, 181-212, 1989.

[16] W. Rachowicz, L. Demkowicz, "An *hp*-Adaptive Finite Element Method for Electromagnetics - Part II: a 3D Implementation", *International Journal for Numerical Methods in Engineering* **53**, 147-180, 2002.

[17] R. Rannacher and F. T. Stuttmeier, "A-Posteriori Error Control in Finite Element Methods via Duality Techniques: Application to Perfect Plasticity" *Comp. Mech.* **21**, 123-133, 1998.